Optimization of over-summer snow storage at mid-latitude and low elevation

Hannah S. Weiss[1], Paul R. Bierman[1,2], Yves Dubief[3], Scott Hamshaw[4]

[1]Rubenstein School for the Environment and Natural Resources, University of Vermont, Burlington, 05401, USA
[2]Geology Department, University of Vermont, Burlington, 05401, USA
[3] Department of Mechanical Engineering, University of Vermont, Burlington, 05401, USA
[4]Department of Civil & Environmental Engineering, University of Vermont, Burlington, 05401, USA

Correspondence to: Hannah S. Weiss (hsweiss@uvm.edu)

Abstract. Climate change, including warmer winter temperatures, a shortened snowfall season, and more rain-on-snow events, threatens nordic skiing as a sport. In response, over-summer snow storage, attempted primarily using wood chips as a covering material, has been successfully employed as a climate change adaptation strategy by high-elevation and/or high-latitude ski centers in Europe and Canada. Such storage has never been attempted at a site with both a low altitude and latitude, and few studies have quantified snowmelt repeatedly through the summer. Such data, along with tests of different cover strategies, are prerequisites to optimizing snow storage strategies. Here, we assess the melt rates of two wood-chip covered snow piles (each ~200 m^3) emplaced during spring 2018 in Craftsbury, Vermont (45° N and 360 m asl) to develop an optimized snow storage strategy. In 2019, we tested that strategy on a much larger, 9300 m^3 pile. In 2018, we continually logged air-to-snow temperature gradients under different cover layers including rigid foam, open cell foam, and wood chips both with and without an underlying insulating blanket and an overlying reflective cover. We also measured ground temperatures to a meter depth adjacent to the snow piles and used a snow tube to measure snow density. During both years, we monitored volume change over the melt season using terrestrial laser scanning. In 2018, snow volume loss ranged from -0.29 to -2.81 m^3 day^{-1} with highest rates in mid-summer and lowest rates in the fall; mean melt rates were 1.24 and 1.50 m^3 day^{-1}, 0.6 to 0.7 % of initial pile volume per day. Snow density did increase over time but most volume loss was the result of melting. Wet wood chips underlain by an insulating blanket and covered with a reflective sheet was the most effective cover combination for minimizing melt, likely because the surface reflected incoming shortwave radiation while the wet wood chips provided significant thermal mass, allowing much of the energy absorbed during the day to be lost by long-wave emission at night. The importance of pile surface area to volume ratio is demonstrated by the melt rates of the 9300 m^3 pile emplaced in 2019 which lost only <0.16% of its initial volume per day between April and September, retaining 65% of the initial snow volume over summer. Together, these data demonstrate the feasibility of over-summer snow storage at mid-latitudes and low altitudes and suggest efficient cover strategies.

1 Introduction

Earth's climate is warming (Steffen et. al., 2018). This warming is expressed not only in warmer nights and days but also in the number of winter rain and thaw events that degrade snow packs (Climate Central, 2016). The duration, extent, and thickness of lake ice and snow have both decreased over the past several decades in response to increasing temperatures, especially at high latitudes (Hewitt et. al., 2018; Sanders-DeMott et. al., 2018). Winter recreation is particularly vulnerable to such warming. The ski industry has responded by increasing snowmaking as well as attempting to reduce melt by covering snow using various materials (Scott and McBoyle, 2007; Pickering and Buckley, 2010; Steiger et. al., 2017). Over the past several decades, the ski industry has improved snow-making strategies and facility operations both to maintain financial stability and to decrease

their output of greenhouse gases (Koenig and Abegg, 1997; Moen and Fredman, 2007; Tervo, 2008; Kaján and Saarinen, 2013). Recent research focuses on analyzing and optimizing stages in the snow production cycle to assist industry efforts (Hanzer et. al., 2014; Spandre et. al., 2016; Grünewald and Wolfsperger, 2019).

Many sites organizing major winter sports events, such as cross-country or alpine world cup races, have adopted over-summer snow storage in response to the unpredictability of snowmaking weather conditions. In areas of high humidity and warm average fall temperatures, summer snow storage is more reliable than expecting weather conditions to be sufficiently cold and dry for making snow at the start of the winter ski season. For example, the 2014 Olympic games at Sochi relied on 750,000 m^3 of stored snow (Pestereva, 2014).

Historically, stored ice provided summer refrigeration. For example, ice houses stored large blocks of lake ice beneath sawdust over the summer (Nagnengast, 1999; Rees, 2013). Today, the ski industry uses stored snow to support the early winter ski season. Modern over-summer snow storage (sometimes referred to as "snow-farming") begins with the creation of snow piles during winter months. Piles are covered (often with sawdust or wood chips and sometimes geotextiles) before the snow is stored over the summer (Skogsberg and Lundberg, 2005). In the fall, the pile is uncovered and snow spread onto trails. Nordic ski centers require less snow-covered area to open than downhill ski centers and so snow storage on the scale of thousands of cubic meters is practical and cost-effective, allowing the center to open on time, instead of losing business if unable to make snow and thus opening later.

Snow storage has been employed predominately at high elevation and/or high latitude ski centers (Fig. 1) many of which benefit from cool, dry summers that minimize energy transfer to the snow, increase evaporative cooling, and thus slow snowmelt. Here, we examine the feasibility of snow storage in the northern United States at a mid-latitude, low altitude (45° N and 360 m asl) site with a humid, temperate climate including warm summer temperatures and high relative humidity which limits evaporative cooling (Fig. 1). Out of the 26 known snow storage locations, our study location has the highest average June-July-August temperature (24 °C) and highest solar radiation levels (Worldclim.org, 2019). We report data on the melt rate of snow stored over the summer and consider those data in the context of both ground temperature and meteorological data that together help define the energy flux responsible for melt into and out of the snow piles. The goals of this research are to: 1) determine the melt rate of small experimental snow piles, 2) suggest an optimized snow storage strategy based on those data, and 3) test the optimized strategy on a larger snow pile sufficient for ski area opening. Our data fill a research gap in measurements of stored snow melt rates and provide a novel case study for snow storage at low altitude and mid-latitude.

2 Background

Although the physics of snowmelt has been considered extensively (Dunne and Leopold, 1978; Horne and Kavaas, 1997; Jin et. al., 1999), there has been limited application of physical and energy transfer knowledge to the problem of over-summer snow storage (Grünewald et. al., 2018). Snowmelt occurs when the snowpack absorbs energy sufficient to raise snow temperature to the melting point (0° C), and then absorbs additional energy to enable the phase change from solid to liquid water (0.334 MJ kg^{-1}). The snowpack gains energy from incoming short- and long-wave radiation, sensible and latent heat transfer from condensation of atmospheric water vapor and cooling and refreezing of rain water, conduction from the underlying ground, and advective heat transfer from wind (Dunne and Leopold, 1978). Loss of energy from the snow pack occurs through convective and conductive heat transfer to the air, evaporative cooling, and long-wave emission to the atmosphere.

Both regional and local climatic factors influence the energy balance of snow. Shortwave radiational gain is related to latitude (highest near equator and least near the poles), time of year (greatest in summer and least in winter), snow pile surface albedo, slope and aspect, as well as cloud and tree canopy cover. Longwave radiation balance depends on atmospheric emissivity, cloudiness, vegetation cover, and temperature of the snow pile surface. Rain falling on the snowpack transfers heat. Conductive heat transfer from the ground depends on soil thermal conductivity and temperature (Kane et. al., 2000; Abu-Hamdeh, 2003). Snow melt typically varies on a diurnal cycle with melt increasing after sunrise, peaking in the afternoon, and decreasing after sunset (Granger and Male, 1978). Once surface melt occurs, water either refreezes if it percolates into a sub-freezing snowpack, flows through an isothermal (0° C) snowpack and then infiltrates into the ground below, or flows along the ground surface below the pile depending on soil infiltration rate (Schneebeli, 1995; Ashcraft and Long, 2005).

Recent research at nordic ski centers in Davos, Switzerland and Martell, Italy (Grünewald et al., 2018) has applied snowmelt physics to optimize over-summer snow storage at high elevation (~1600 m) and mid latitude (~46° N). The Davos location has an average summer relative humidity of 79%. Each nordic center built piles of machine-made snow and covered them with 40 cm of wet sawdust and wood chips; researchers then used utilized terrestrial laser scanning to measure the initial (spring) and final (fall) volumes of the two piles. These snow piles retained 74% and 63% of their volume over the summer. Using a physically based model, Grünewald et al. suggested that the most effective cover, in relation to work and cost, was a 40 cm thick layer of mixed wet sawdust and wood chips, which reduced energy input into the pile by a factor of 12 (1504 MJ m^{-2} without wood chips as opposed to 128 MJ m^{-2} with wood chips). Deeper cover layers can save more snow but costs are higher. During the day, solar radiation caused evaporation from surface wood chips while capillary flow continually supplied moisture from the melting snow to the surface. The wet wood chips/sawdust also provided a thermal mass slowing the transfer of energy from the surface to the snow beneath.

Lintzén and Knutsson (2018) reviewed current knowledge of snow storage and experience from areas in Scandinavia and reported new results from an experiment in northern Sweden, analyzing melt loss of stored snow. They report that the most common snow storage method employs a breathable surface layer over an insulating material. From field observations at multiple nordic ski centers, they have found that the choice and age of covering affects melt rate; older wood chips were less effective at reducing melt than fresh chips. Lintzén and Knutsson also determined that wood chips were a more effective cover than bark. They measured snow volumes three times over the summer and found that higher relative humidity increased melt rate. They also investigated the geometry of snow piles and determined that shaping piles in a way that maximized volume to surface area minimized melt loss; however, steeper snow pile sides caused sliding and failure of cover materials (Lintzén and Knutsson, 2018).

Data related to snow storage for the purpose of summer cooling to improve energy efficiency and comfort supplements those gathered from ski centers. In central Sweden, the Sundsvall Hospital conserves snow over the summer for air conditioning with a 140 m x 60 m storage area (holding 60,000 m^3 snow) underlain by watertight asphalt (Nordell and Skogsberg, 2000). After covering with 20 cm of wood chips, the majority of natural snowmelt resulted from heat transfer from air (83%), while heat transfer from groundwater drove 13% of melt and heat from rain accounted for 4% of melt. Similar work was done by Kumar et. al., (2016) and Morofsky (1982) in Canada, and by Hamada et. al. (2010) in Japan.

3 Methods and Setting

3.1 Study Location

We conducted our experiment at the Craftsbury Outdoor Center (COC), a sustainability-focused, full year recreation venue located in northeastern Vermont at 360 m asl (Fig. 1), an area with warm, humid summers and cold dry winters. Average maximum monthly air temperature at St. Johnsbury, VT (closest National Oceanic and Atmospheric Administration (NOAA) station to the COC about 30 km southeast, at 215 m asl) between 1895 and 2018 ranges between 3.6° C (January) and 29° C (July), mean temperatures range from -8.3° C (January) to 20.7° C (July), and minimum air temperature ranges between -34° C (December) and 15° C (July). Soils in the area, are very rocky, silty loam, sandy loam, and loam developed on glacial till (USDA, 2019). Average annual summer precipitation is ~300 mm (NOAA, 2019). The most common landcover types are forest and woodlands (USGS, 2019). The COC maintains 105 km of groomed nordic ski trails and hosts national and international races several times each winter.

3.2 Initial Snow Pile Experiments

On March 30, 2018, two snow piles were emplaced at the COC using Piston Bully snow groomers at two separate sites (Fig. 2). Site 1 is adjacent to the COC's main campus buildings in direct sunlight, with minimal wind protection. Site 2 is 1 km north of Site 1, within a cleared depression in the forest also in direct sunlight, but more protected from wind than Site 1. At the time of emplacement, the snow was transformed and had a density of >500 kg m^{-3} (see section 3.5 for snow density measurement methods). At site 1, 225 m^3 of machine-made snow was banked against a north-facing slope. At site 2, 210 m^3 of natural snow was shaped into symmetrical, rounded pile. The two piles were draped with thin sheets of clear plastic. The plastic sheets, about 0.15 mm thick, were impermeable, and emplaced to prevent wood chips from mixing with the snow. The piles were then covered with an irregular layer of wood chips averaging 20 ±10 cm (1 SD) on April 21, 2018.; chip thickness ranged from a minimum of 6 cm to a maximum of 40 cm, (Fig. 3). In early July, about 50 m^3 of snow was removed from the pile at site 1 by COC personnel, the plastic was removed, and the remaining snow was covered again with wood chips and left for continued monitoring.

3.3 Weather Stations

Weather stations adjacent to each pile and 3-4 m above the ground surface, (Davis Vantage Pro 2) collected air temperature, humidity, precipitation, solar radiation, wind speed/direction, and barometric pressure data. The weather stations record data at 15-minute intervals and transfer them to the web where they are publicly accessible (wunderground.com/personal-weather-station/dashboard?ID=KVTCRAFT2#history). Local soil temperature was measured with temperature sensors installed at four depths within the soil (5 cm, 20 cm, 50 cm and 100 or 105 cm below the surface) adjacent to each snow pile. Two HOBO Onset dataloggers recorded temperatures at four depths at 20-minute intervals between June, 2017 and October, 2018.

3.4 Terrestrial Scanning Field Methods and Processing

During spring and summer, the shape and volume of the piles were measured every 10-14 days using a terrestrial laser scanner (Reigl VZ-1000)). Terrestrial laser scanning (TLS) is a highly accurate method for obtaining digital elevation models (DEMs) of various terrain types, including snow surfaces (Prokop et al., 2008; Molina et al., 2014). Six to ten permanent tie-points around each pile were established during the initial survey by fastening reflective 5 cm disks to stable surfaces such as large trees and buildings. The first survey was done prior to snow pile placement in order to establish ground surface topography. Tie-point locations were determined and fixed relative to the scanner GPS position during the initial scan. Each survey consisted of three or four scans per site (depending on available vantage points), which were combined in the RiSCAN Pro

software (v 2.6.2). Scan registration was done in RiSCAN using a combination of tie-point registration (finding corresponding points), and the multi-station adjustment routine using plane patches and tie-objects. Similar studies of monitoring bare and covered snow surfaces with TLS have applied this technique (Prokop et al., 2008, Grünewald et al., 2018, Grünewald and Wolfsperger, 2019). Scans were collected at a horizontal and vertical angular resolution of 0.08. Scans were collected from distances less than 100 m resulting in average point spacing over the pile <1 cm.

To calculate snow pile volumes and volumetric change over time (between scans), point-clouds of each pile were processed into DEMs. Processing workflow involved cropping the point-cloud to the area of interest in RiSCAN Pro and exporting cropped point-clouds into .las format, projected into Vermont State Plane NAD83 coordinates. Point-clouds were converted to a 10 cm resolution DEM using the min-Z filter and QT Modeler software (v. 8.0.7.2) and adaptive triangulation to fill in small data gaps. Volume calculations and differences in volume between sequential surveys were calculated in QT Modeler using these DEMs.

3.5 Density

Snow density was measured using a Rickly Federal Snow Sample Tube. The snow tube was weighed, pushed into the snow, removed, and weighed again. The weight of the tube was subtracted from the combined weight of the snow and tube, and density calculated by dividing the mass of snow by the volume (length of snow within the tube multiplied by the area of the opening, ~13 cm^2). Density was collected three times throughout the summer in March, May, and July at the top surface of pile 1 during 2018. In 2019, density was collected once at the top of the snow pile in February.

3.6 Cover Experiments

Cover experiments were performed at both sites in June and July, 2018. At site 1, two 5-cm-thick, impermeable, rigid foam boards (R=3.9 per 2.5 cm, value expressing resistance to conductive heat flow) were stacked and compared to a 20 cm, uniform, porous layer of wood chips both with and without a reflective cover (aluminized space-blanket). At site 2, we covered snow with a double layered, 2.5 cm thick insulating concrete curing blanket (R=3.3 per 2.5 cm) and overlaid the blanket with either open-cell, permeable foam (R=3.5 per 2.5 cm) or a uniform, porous layer of wood chips (20 cm height) both with a reflective cover. For both foam experiments, wood chips and plastic sheeting were removed from the test area. For wood chip experiments, plastic sheeting was removed from the test area. Individual cover experiments were conducted in areas of 1 m^2 each, with thermosensors placed in the center of each quadrat at varying depths between layers (Fig. 4).

3.7 Power Spectral Density Function

We compute the Power Spectral Density function (PSD) to determine relative effectiveness of the different covers. The temperature signal is first decomposed in a series of waves of well-defined frequencies:

$$T(t)=\frac{1}{N}\sum_{k=0}^{N-1}\hat{T}_k \exp\left(i2\pi f_k t\right) \quad (1)$$

where $\hat{T}_k$ is the Fourier mode at frequency $f_k = k/2\Delta T$, $1/\Delta T$ is the sampling frequency of temperature acquisition, and N is the number of samples in the time series. The Fourier mode contains both amplitude and phase information for each wave. The PSD is the power of the signal,

$$\mathrm{PSD(T)}=\frac{\Delta t}{N}\sum_{k=0}^{N-1}\left|\hat{T}_k\right|^2 \quad (2)$$

which is the sum of the contributions of each wave to the power (or variance) of the signal. Typically plotted on a log-log plot, the norm of the Fourier modes as a function of frequencies is a powerful tool to detect dominant frequencies (Welch, 1967). In the summer, the dominant oscillation in temperature is diurnal; thus, using PSD, we can judge the effectiveness of cover materials by their ability to damp the diurnal temperature signal and relevant harmonics. We computed the PSD for all temperature records in selected cover experiments (Fig. 4, panels b, e, f).

3.8 Validating Cover Method, Summer 2019

Based on data collected during summer 2018, the COC chose site 2 (Fig. 2) as their snow storage site. Based on cost and ease of installation, they chose a two layer cover system, a uniform layer of wood chips with a reflective covering. The pile filled a former oblong pond basin and was gently sloped. During February, machine-made snow was blown into the pile using fan-less snow making wands. Snow density at and just after emplacement was high, ranging between 500 and 600 kg m^{-3}. In March, the snow pile was shaped and further compacted with Piston Bully groomers and excavators; at that time, LiDAR showed the pile had a volume of about 9300 m^3, without wood chips. During the next 6 weeks, the snow pile was allowed to compact and grow denser. In late April, the pile was partially covered in woodchips. By the end of May, the snow pile was completely covered in wood chips (total ~ 650 m^3). Using the exposed surface area of the pile without wood chips (2300 m^2) and the volume of woodchips, we calculate the average woodchip thickness to be 28 cm. By the end of June, the snow pile was covered in a white, 75% reflective and breathable Beltech 2911 geofabric, secured by ropes and rocks to prevent wind disruption. Between March and September, the pile was scanned using LiDAR every two weeks and processed using methods described in section 3.4.

4 Results

4. 1 Meteorological Data/Ground Temperature Data

Climate at the COC is strongly seasonal – such seasonality is clear in the meteorological data collected between June, 2017 and October, 2018 (Fig. 5). Between June 2017 and October 2018, air temperature varied between -28.2 and 33ºC (mean annual temperature = 6 ºC). Precipitation fell at a maximum rate of 22 mm day^{-1} (mean 0.06 mm day^{-1}) and relative humidity ranged between 14%-93% (mean 78 ± 15%). Solar radiation had a 24-hour average of 109 W m^{-2} and maximum of 1144 W m^{-2}. Air temperature and solar radiation followed similar trends over the sixteen months, decreasing during winter months and increasing during summer months. Precipitation did not follow any significant pattern, relative humidity remained high (NOAA classifies above 65% as high and relative humidity remained above this level for the summer), varying more during summer than winter months. Average summer temperature in 2018 (June, July, and August 2018, 22.4 ° C) was ranked by NOAA as “Much above the average of 20.7° C”; in 2019, average summer temperature ranked “Above Average” (21 ° C). Both years had near average precipitation (NOAA, 2019; wunderground.com, 2019).

Ground temperature from all four depths at both locations followed similar trends. The shallowest sensor (5 cm below the surface) recorded the greatest variance over time (SD = 7.4° C for site 1). Ground temperature variations decreased in amplitude as soil depth increased; at 1 m in depth, the atmospheric temperature signal was damped (SD = 3.9° C for site 1). Ground temperatures for all depths showed consistent warming from installation (June 11, 2017) through late August 2017 and then decreased through February 2018. The shallowest sensor revealed slight warming after February while the deeper

sensors remained stable until May 2018. During May, warming increased more noticeably for all four sensors. Ground temperature depth trends inverted during both May and November. During the winter, the coldest temperatures were at the surface; during summer, the coldest temperatures were at depth. Figure 5 displays data from sensors adjacent to pile 1 – data were collected at both sites but are missing from Site 2 between December 12, 2017 and April 21, 2018.

4.2 Snow Volume/Density

Snow in both 2018 piles lasted until mid-September; however, snow volume decreased consistently throughout the summer (Fig. 6, Fig. 7). Comparing the laser scan survey completed just after wood chip emplacement, with the initial bare snow survey, showed that the layer of chips ranged in depth from 6-40 cm, with an average of 19±11 cm for pile 1 and 21±11 cm (1 SD) for pile 2 (Fig. 3). After adding wood chips, snow volume in both piles decreased following similar trends (Fig. 6); initial decreases in volume were partly related to compaction and increases in snow density as snow density was ~ 500 kg m^{-3} at emplacement, 600 kg m^{-3} in May, and 700 kg m^{-3} in July. Relative to newly fallen snow (100-200 kg m^{-3}), the snow in these piles was closer in density to ice (900 kg m^{-3}). These measurements are supported by qualitative observations of changes in snow crystal morphology over the summer (increased rounding), size (up to 5 mm by July), increasing wetness (higher liquid water content), and clarity (from white to clear by summer's end). Continued volume loss over the summer was predominately the result of melt. Average rates of volume change for both piles were relatively similar (1.24 m^3 day^{-1} and 1.50 m^3 day^{-1}) representing 0.6 to 0.7 % of initial pile volume per day. Maximum loss rates, recorded in July, reached 1.98 m^3 day^{-1} and 2.81 m^3 day^{-1} (Fig. 7.) As summer shifted into fall, loss rate decreased (Fig. 7). Minimum rates of change for both piles occurred in September and were 0.29 m^3 day^{-1} and 0.88 m^3 day^{-1}.

As the piles decreased in volume over the summer, crevasses formed along the edge of the plastic sheeting, which exposed the snow to direct sunlight and thus increased melt rates. We did not observe meltwater around either of the piles suggesting melt occurred at a rate which allowed for infiltration into the rocky sandy loam soil below. The woodchips deeper in the cover remained cold and wet throughout the summer while the woodchips on the surface were consistently dry in the absence of rainfall.

4.3 Cover Experiments

Thermal buffering is a function of air temperature, longwave emissions, and turbulent fluxes. We chose temperature at the snow/cover interface to indicate cover efficiency because all experiments were subjected to similar external conditions and because we have continuous data series of temperature at depths in, above and below the cover during each of the experiments. Two experiments preformed on 1 m^2 plots on each snow pile revealed that different combinations of cover materials resulted in a variety of cover efficiencies (Fig. 4). Each experiment lasted about a week and took place in June and July, respectively. We assessed cover efficiency by determining which material combination maintained the lowest and steadiest temperature at the snow-cover interface and which most effectively damped the diurnal temperature signal (detected using PSD analysis). For all panels (Fig.4), temperature ranges at the snow-cover interface (blue line) are (a) 0.21– 4.33◦C, (b) -0.04 – 3.69◦C, (c) -0.22 – 44.57◦C, (d) -0.09 – 9.86◦C, (e) 0.47 – 23.89◦C, (f) 0.04 –2.44◦C. On the rigid foam, open-celled foam, and wood chip plots, the highest temperature was measured in air above the surface (max = 41.2° C, Fig. 4 panel f). During this first experiment, air temperatures above the reflective blanket were higher than above the non-reflective surface. When all plots were covered with a reflective blanket, all air temperatures above the pile were similar; yet, temperatures at lower depths, under different cover materials (wood chips and open cell foam) varied significantly. The lowest and most stable temperatures

at the snow/cover interface resulted when the stored snow was covered directly with an insulating concrete curing blanket, then 20 cm of wet wood chips, and finally by a reflective sheet.

4.6 Power Spectral Density

The dominant frequency in all our records is diurnal as expected (Fig. 8). The air sensors at 46 cm (yellow lines) also measure significant contributions of harmonics at periods of 12 h, 6 h and 3 h (peaks at 10^{0}, $10^{0.1}$, $10^{0.2}$, Fig. 8). These harmonics can also be detected in temperature records collected at different depths in the cover materials with various relative strengths. In the foam cover experiment (b), the diurnal frequency and its harmonics are detectable in all layers; however, the three-layer system (insulating blanket, wet wood chips, and reflective cover, panel 8c) fully damps all oscillations, as shown by the flatness of the PSD below the cover. In the absence of an insulating blanket, the two-material cover system (reflective cover and wood chips) is slightly less efficient at damping the diurnal oscillation (Fig. 8 a).

4.7 Summer 2019

The 9,300 m^3 snow pile emplaced in 2019 lost volume at an average rate of 15 m^3 day^{-1} (min= 5 m^3 day^{-1} in early July, max = 25 m^3 day^{-1} in between April and May, when the snow pile was compacting and being covered by wood chips). Between the initial LiDAR survey in March and the last survey in September, the pile lost 2,460 m^3 of snow, a 35% volume loss (not including wood chips). The average percentage loss per day was 0.16% of the initial volume.

5 Discussion

Data collected during this research allow us to: 1) determine the melt rate of small snow piles stored over summer with different coverings, 2) suggest an optimal snow preservation strategy for low elevation, mid latitude sites based on these data, and 3) test this optimized snow storage strategy at scale.

5.1 Experimental snow pile melt rate

The survival of small (200 m^3) snow piles through the warmer than average summer of 2018 and the results of both repeated LiDAR surveys and continuous in situ thermal data collected during a variety of different snow cover experiments, suggest ways to optimize snow over-summer snow storage at low elevations and mid latitudes. The 2018 snow piles experienced non-uniform cover, non-ideal geometry, and developed crevices that exposed snow to direct sunlight; all of which increase melt rate. Field observations and LiDAR surveys demonstrated that the thickness of wood chips covering the snow was not uniform and became less uniform over time as melt changed pile shape (Fig. 3). Wood chip depth changed over the summer as crevices, which grew over time, exposed bare snow to direct sunlight which led to rapid and non-uniform pile melting. Crevices formed along boundaries of the large plastic sheets, which were emplaced to prevent woodchips from mixing with the snow. Openings in the wood chip cover also resulted from snow slumping within the pile – both piles had steep sides and the LiDAR DEMs revealed snow moving downslope (Fig. 6). Lintzén and Knutsson (2018) reference similar snow pile/cover failure due to steep pile-side geometry.

Snow pile size likely impacts melt rate significantly. The two test piles were small, only a small percent of the volume of snow typically stored over summer by Nordic ski areas. For example, in Davos, Switzerland and Martell, Italy, test piles were about 6000 m^3 and 6300 m^3 (Grünewald et. al., 2018). The Nordkette nordic ski operation in Innsbruck, Austria stores ~13,000 m^3 of snow and Ostersund, Sweden stores 20,000 to 50,000 m^3 piles. Small piles have a larger surface area to volume ratio (SA/V),

which allows more effective heat transfer through radiation, conduction and latent heat transfer. A simple comparison of two hemispheres, one containing 200 m^3 of snow and the other containing 20,000 m^3 of snow indicates that SA/V changes from 0.43 to 0.04 between the smaller and larger pile. As larger piles have a lower SA/V ratio in comparison to smaller piles, there is comparatively less snow near the surface thermal boundary, which decreases melt rate.

5.2 Optimal approach for over-summer snow preservation at mid-latitude and low elevation

The survival of snow through the summer in small piles and with simple, wood chip, foam and reflective coverings, suggests that larger piles, using an optimized cover strategy, will allow for practical over-summer snow storage at mid-latitude (< 45° N) and low-altitude (< 350 m asl) locations. Previous snow storage studies found success with woody covers as well. Grünewald et. al., (2018) suggested that a 40 cm layer of sawdust sufficiently optimized snow retention in Davos, Switzerland and Martell, Italy. Skogsberg and Nordell (2001) reported that wood chips reduced snowmelt by 20-30% at the Sundsvall Hospital in Sweden. Lintzén and Knutsson (2018) built snowmelt models and ran field tests in northern Scandanavia, revealing that thick layers of woody materials successfully minimized snowmelt. Our results are encouraging given the relative warmth of the 2018 summer season, the simple and spatially inconsistent nature of our cover material (20±10 cm of woodchips), and the small size of the test piles (~200 m^3).

The experimental data (Fig. 4), show that the magnitude of daily temperature oscillations at the snow surface below the covering (blue line in all panels) is highly dependent upon the cover strategy. For example, in Figure 4c, the temperature within the rigid foam board increases above air temperature (purple line increasing above the yellow line). Due to the rigidity of the foam boards and the non-uniform melting of the pile, the foam shifted and exposed snow to direct solar radiation, as well as allowed warm air to move between the snow and the foam. Such failure of the cover system allowed temperatures at the snow interface to rise significantly above 0 ◦C. The three-layer cover (insulating blanket, wet wood chips, and reflective cover) minimizes heat transfer into the stored snow as evidenced by the lack of diurnal temperature oscillations at the snow surface during this and only this experiment (Fig 4e). The comparison between foam and saturated wood chips PSDs (Fig. 8) show the dramatic effect on the heat transfer from the atmosphere to the snow caused by the high heat capacity and thus thermal inertia of wet wood chips. The damping of diurnal temperature peaks by the three layer cover system suggest it will be the most effective for preserving snow over the summer.

Although the relevant heat transfer mechanisms remain uncertain, Figure 8 demonstrates the effectiveness of the three layer cover approach to buffering heat transfer from the environment to the snow. Deducing specific heat transfer mechanisms will require different and more complex measurements, as heat transfer is dependent upon not only air temperature, but also surface temperature, long-wave radiation, and turbulent fluxes. Perhaps, evaporation of water from the wet wood chips absorbs thermal energy during the day which is released as the latent heat of condensation at night when the reflective blanket cools – effectively increasing the thermal mass of the wood chip layer. Depending on weather conditions, which influence long-wave radiation through cloudiness and turbulent fluxes through wind, the heat transfer may be directed toward the snow pile (warm nights) or radiated to the atmosphere (cold nights). In any case, the large thermal mass of wet wood chips, in concert with an underlying layer (the concrete curing blanket), and rejection of shortwave incident radiation from sunlight by the reflective cover, appears more important than the insulating capability (R-value) of the cover material in damping daily temperature fluctuations at the snow surface.

5.3 Summer 2019, Testing the Optimized Snow Storage Strategy at Scale

Field data, LiDAR, and thermal observations from the 2018 experiments allowed for a full scale test of our optimized snow storage strategy in 2019. Optimization began by further excavating the storage area so the resulting pile would sit within a pit and have gently sloping sides. Snowmaking was done so that the density of the snow emplaced was already high to minimize settling after covering. The snow was then compacted by repeated passes of large excavators and Piston Bully groomers. Letting the snow settle and transform before covering reduced the chance of mass movements compromising the pile and cover integrity. Rather than use metallized cover material, which was expensive, fragile and impermeable, we used a high albedo (0.75) white, permeable geofabric that allowed rain to infiltrate, thus mitigating regulatory concerns related to a large impermeable area.

The 2019 data validate the optimization approach suggested by the 2018 experiments. The most rapid volume loss in 2019 was early in the melt season as the snow in the pile transformed and compacted; rates of volume loss later in the summer, while higher in absolute terms than those in 2018 because the pile was 45 times larger, were more than three times lower in percentage terms. Compared with the average percentage loss per day of the 2018 piles (0.55% per day), the 2019 snow pile average percentage loss per day was 0.16%. We suspect that the difference in volume loss reflects primarily the surface area to volume ratio of the 2019 snow pile which is about 2 times greater than the small piles tested in 2018. Other factors may also be important. The complete covering of the 2019 pile with a reflective geofabric likely slowed melt by rejecting shortwave radiation as well as protecting the snow even if the wood chips shifted. LiDAR imagery from 2019 demonstrates that gentle side slopes of the pile prevented any large mass movements of snow indicating that pile shape and pre-consolidation are important.

LiDAR data show that from April until September, more than 65% of the snow initially placed in the 2019 pile remained. Using the snow density from 2018, which increased from 500 to 700 kg m^{-3} over the summer, much of this volume loss could be accounted from by compaction rather than melting. This suggestion is supported by the lack of surface water draining from the pile, which is underlain by relatively impermeable rock and clay-rich glacial till. With September temperatures and sun angle dropping, incident solar radiation as well as convective and conductive heat transfer are diminished greatly from mid-summer values. This means that the COC will have > 5000 m^3 of snow to spread in November for early season skiing. Covering 5 meter wide trails 50 cm deep will allow at least 2 km of skiing at opening as well as providing a base so that any natural snow that does fall will be retained.

6 Conclusions

Data presented here show that snow storage at mid latitudes and low altitudes is a practical climate change adaptation that can extend the nordic ski season and the sport's viability as the climate continues to warm. Using 14 terrestrial laser scans between March and September, 2018, we determined melt rates of two, 200 m^3 snow piles covered in wood chips. Average volume loss rates were 1.24 m^3 day^{-1} and 1.50 m^3 day^{-1}, with highest melt rates in July and lowest melt rates in September. A three-layer cover approach was most effective: concrete curing blanket, a 20 cm layer of woodchips, a reflective covering. This cover approach reduces solar gain and buffers the effect of >30° C summer daytime temperatures and high (>78%) relative humidity on stored snow. Using data collected during summer 2018, we tested our experimental results in summer of 2019 by creating a 9300 m^3 snow pile. Due to cost and logistical issues, we covered the pile using a two layer approach - 650 m^3 of woodchips and white, permeable geofabric. The volume loss rate between March and September was 15 m^3 day^{-1} (or 0.16% of the initial volume per day) which provided ~ 6100 m^3 of snow at the end of the summer. This quantity of snow is sufficient

for the COC to open their 2019 season and represents >65% retention of snow by volume, comparable to storage losses at other storage sites (at higher altitude and latitude).

Data Availability

Data is available at https://doi.pangaea.de/10.1594/PANGAEA.899744

Author Contribution

P. Bierman and Y. Dubief co-conceptualized the experiment. H. Weiss and Y. Dubief curated the data. H. Weiss, Y. Dubief, S. Hamshaw conducted the LiDAR and PSD analysis. H. Weiss and P. Bierman acquired funding, developed the methodology (assisted by S. Hamshaw), conducted the investigation, and validated data. H. Weiss, P. Bierman, and Y. Dubief prepared data visualizations. H. Weiss and P. Bierman wrote the original manuscript draft. All authors contributed to the review and editing process.

Acknowledgements

We thank J. Geer and D. Dreissigacker, directors of the Craftsbury Outdoor Center for supporting this project, the University of Vermont for financial support (including the Graduate College, the Office of Undergraduate Research, the Geology Department, the Rubenstein School for the Environment and Natural Resources, and the Mechanical Engineering Department). Additional support provided by the National Science Foundation under CMMI-1229045. Field work assisted by L. Williams and A. Murtha.

References

Abu-Hamdeh, N. H.: Thermal properties of soils as affected by density and water content, Biosyst. Eng., 86, 97-102, doi:10.1016/S1537-5110(03)00112-0, 2003.

Ashcraft, I. S. and Long, D. G.: Differentiation between melt and freeze stages of the melt cycle using SSM/I channel ratios, IEEE T. Geosci. Remote, 43, 1317-1323, doi:10.1109/TGRS.2005.845642, 2005.

Climate Central: available at: https://www.climatecentral.org/news/winters-becoming-more-rainy-across-us-20017, 2016, last access: 10 August 2019

Climate Summary for Saint Johnsbury, VT: available at: https://www.fairbanksmuseum.org/eye-on-the-sky/summaries-for-st-js-climate/normals-and-extremes, last access: 6 February, 2019.

Craftsbury Outdoor Center KVTCRAFT2:available at: https://www.wunderground.com/personal-weather-station/dashboard?ID=KVTCRAFT2#history, last access: 12 December 2018.

Dunne, T., and Leopold, L.: Snow Hydrology, in: Water in environmental planning, WH Freeman and Company, New York, 465-483, 1978.

Geologic units in Orleans county, Vermont: available at: https://mrdata.usgs.gov/geology/state/fips-unit.php?code=f50019, last access: 15 October, 2018.

Granger, R. J., and Male, D. H.: Melting of a prairie snowpack, J. Appl. Meteorol. Clim., 17, 1833-1842, doi:10.1175/1520-0450(1978)017<1833:Moaps>2.0.Co;2, 1978.

Grünewald, T., Wolfsperger, F.: Water losses during technical snow production: results from field experiments, Front. Earth Sci.,7:78, 1-13, doi:10.3389/feart.2019.00078, 2019.

Grünewald, T., Wolfsperger, F., and Lehning, M.: Snow farming: conserving snow over the summer season, Cryosphere, 12, 385-400, doi:10.5194/tc-12-385-2018, 2018.

Hamada, Y., Kubota, H., Nakamura, M., Kudo, K., and Hashimoto, Y.: Experiments and evaluation of a mobile high-density snow storage system, Energ. Buildings, 42, 178-182, 10.1016/j.enbuild.2009.08.012, 2010.

Hanzer, F., Marke, T., and Strasser, U.: Distributed, explicit modeling of technical snow production for a ski area in the Schladming region (Austrian Alps), Cold Reg. Sci. Technol, 108, 113-124, doi:10.1016/j.coldregions.2014.08.003, 2014.

Hewitt, B. A., Lopez, L. S., Gaibisels, K. M., Murdoch, A., Higgins, S. N., Magnuson, J. J., Paterson, A. M., Rusak, J. A., Yao, H., and Sharma, S.: Historical trends, drivers, and future projections of ice phenology in small north temperate lakes in the Laurentian Great Lakes watershed, Water-SUI, 70,1-16, doi:10.3390/w10010070, 2018.

Horne, F. E., and Kavvas, M. L.: Physics of the spatially averaged snowmelt process, J. Hydrol, 191, 179-207, doi:10.1016/s0022-1694(96)03063-6, 1997.

Jin, J., Gao, X., Yang, Z. L., Bales, R. C., Sorooshian, S., Dickinson, R. E., Sun, S. F., and Wu, G. X.: Comparative analyses of physically based snowmelt models for climate simulations, J. Climate, 12, 2643-2657, doi:10.1175/1520-0442(1999)012<2643:caopbs>2.0.co;2, 1999.

Kaján, E., and Saarinen, J.: Tourism, climate change and adaptation: A review, Curr. Issues Tour., 16, 167-195, doi:10.1080/13683500.2013.774323, 2013.

Kane, D. L., Hinkel, K. M., Goering, D. J., Hinzman, L. D., and Outcalt, S. I.: Non-conductive heat transfer associated with frozen soils, Global Planet. Change, 29, 275-292, doi:10.1016/S0921-8181(01)00095-9, 2000.

Koenig, U., and Abegg, B.: Impacts of climate change on winter tourism in the Swiss Alps, J. Sustain. Tour., 5, 46-58, doi:10.1080/09669589708667275, 2010.

Kumar, V., Hewage, K., Haider, H., and Sadiq, R.: Techno-economic performance evaluation of building cooling systems: A study of snow storage and conventional chiller systems, Cold Reg. Sci. Technol., 130, 8-20, doi:10.1016/j.coldregions.2016.07.004, 2016.

Lintzén, N., and Knutsson, S.: Snow storage–Modelling, theory and some new research, Cold Reg. Sci. Technol., 153, 45-54, 10.1016/j.coldregions.2018.04.015, 2018.

Moen, J., and Fredman, P.: Effects of climate change on alpine skiing in Sweden, J. Sustain Tour., 15, 418-437, doi:10.2167/jost624.0, 2009.

Molina, J.-L., Rodríguez-Gonzálvez, P., Molina, M. C., González-Aguilera, D. and Espejo, F.: Geomatic methods at the service of water resources modelling, J. of Hydro., 509, 150–162, doi:10.1016/j.jhydrol.2013.11.034, 2014.

Morofsky, E.: Long-term latent energy storage – the Canadian perspective, Enrgy Proced., 405-412, doi:10.1016/B978-0-08-029396-7.50056-2, 1982.

Nagnengast, B.: Comfort from a block of ice: a history of comfort cooling using ice, ASHRAE J., Supplement, 49-57, 1999.

National Oceanic and Atmospheric Administration (NOAA): available at: https://www.noaa.gov/, last access: 22 October, 2018.

Nordell, B., and Skogsberg, K.: Seasonal snow storage for cooling of hospital at Sundsvall, 8th International Conference on Thermal Energy Storage, University of Stuttgart, Germany, 2000.

Pestereva, N. M.: Modern engineering technology to adapt to the adverse weather and climatic conditions at mountain ski resorts, Life Sci. J., 11 (9), 800-804, 2014

Pickering, C. M., and Buckley, R. C.: Climate response by the ski industry: the shortcomings of snowmaking for Australian resorts, Ambio, 39, 430-438, doi:10.1007/s13280-010-0039-y, 2010.

Prokop, A., Schirmer, M., Rub, M., Lehning, M. and Stocker, M.: A comparison of measurement methods: terrestrial laser scanning, tachymetry and snow probing for the determination of the spatial snow-depth distribution on slopes, Ann. Glaciol., 49, 210–216, doi:10.3189/172756408787814726, 2008.

Rees, J.: Refrigeration Nation: a History of Ice, Appliances, and Enterprise in America, John Hopkins University Press, Maryland, 248 pp., 2013.

Schneebeli, M.: Development and stability of preferential flow paths in a layered snowpack, IAHS Boulder Symposium, Boulder, United States, July 1995, IAHS Publ. no. 288, 1995.

Scott, D., and McBoyle, G.: Climate change adaptation in the ski industry, Mitig. Adapt. Strat. Gl., 12, 1411, doi:10.1007/s11027-006-9071-4, 2007.

Skogsberg, K.: Seasonal snow storage for space and process cooling, Ph.D, Department of Civil, Environmental and Natural Resources Engineering, Luleå tekniska universitet, 2005.

Skogsberg, K., and Lundberg, A.: Wood chips as thermal insulation of snow, Cold Reg. Sci. Technol., 43, 207-218, doi:10.1016/j.coldregions.2005.06.001, 2005.

Spandre, P., François, H., George-Marcelpoil, E., Morin, E.: Panel based assessment of snow management operations in French ski resorts, J. Outdoor Rec. Tour., 16, 24-36, doi:10.1016/j.jort.2016.09.002, 2016.

Steffen, W., Rockström, J., Richardson, K., Lenton, T. M., Folke, C., Liverman, D., Summerhayes, C. P., Barnosky, A. D., Cornell, S. E., and Crucifix, M.: Trajectories of the earth system in the Anthropocene, P. Natl. Acad. Sci. USA, 115, 8252-8259, doi:10.1073/pnas.1810141115, 2018.

Steiger, R., Scott, D., Abegg, B., Pons, M., Aall, C.: A critical review of climate change risk for ski tourism, Curr. Issues Tour., 22:11. 1343-1379, doi:10.1080/13683500.2017.1410110, 2017.

Tervo, K.: The operational and regional vulnerability of winter tourism to climate variability and change: The case of the Finnish nature-based tourism entrepreneurs, Scand. J. Hosp. Tour., 8, 317-332, doi:10.1080/15022250802553696, 2008.

Web Soil Survey: available at: https://websoilsurvey.nrcs.usda.gov/app/WebSoilSurvey.aspx, last access: 20 October, 2018.

Welch, P., 1967, The use of fast Fourier transform for the estimation of power spectra: a method based on time averaging over short, modified periodograms, IEEE, 15:2, 70-73

Worldclim – Global Climate Data: available at: http://worldclim.org/version2, last access: 14 September, 2019.

Tables

Table 1: Weather parameters measured between June 2017 and October 2018 at the Craftsbury Outdoor Center, Craftsbury VT.

	Air temperature (° C)	Humidity (%)	Precipitation (mm day^{-1})	Solar radiation (W m^{-2})
Minimum	-28	14	0	0
Maximum	33	93	22	1144
Mean	9	79	0.1	109
Standard Deviation	12	15	0.4	205

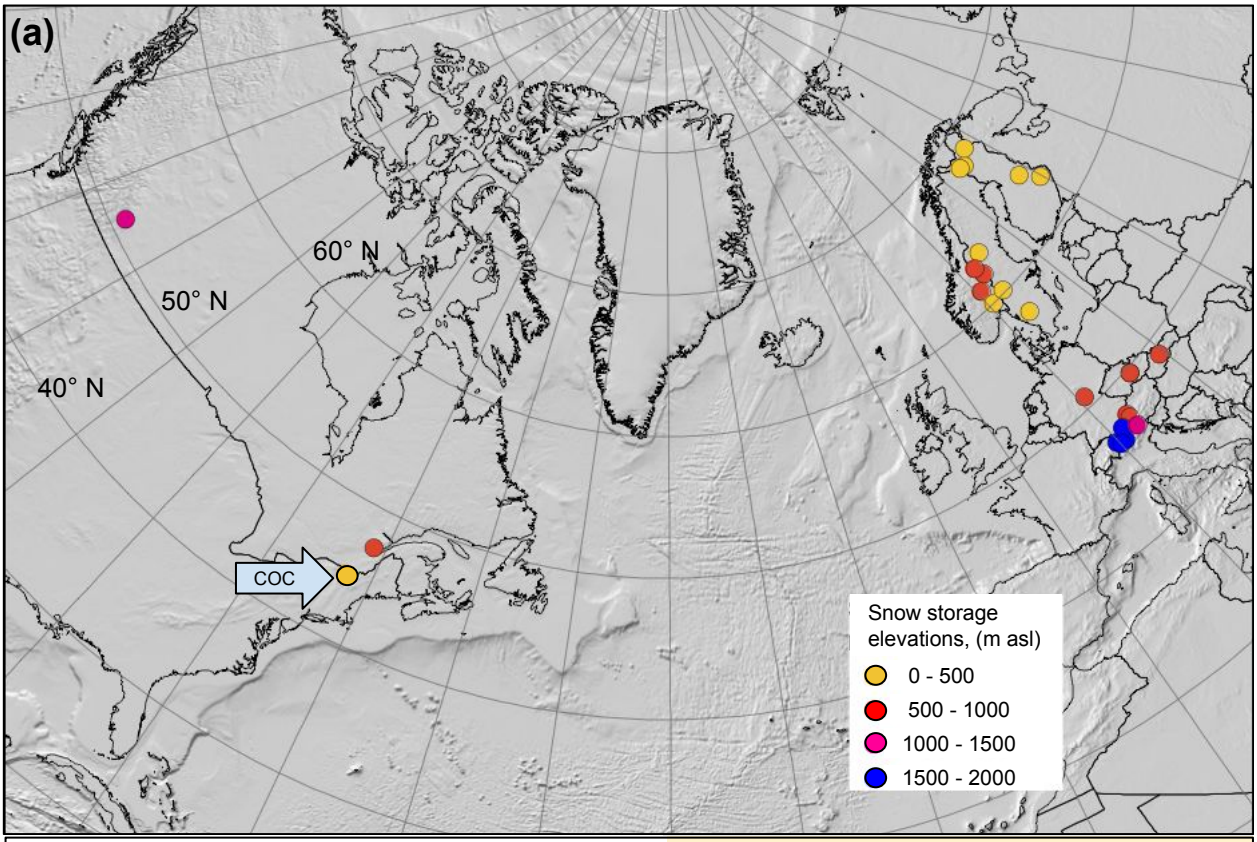

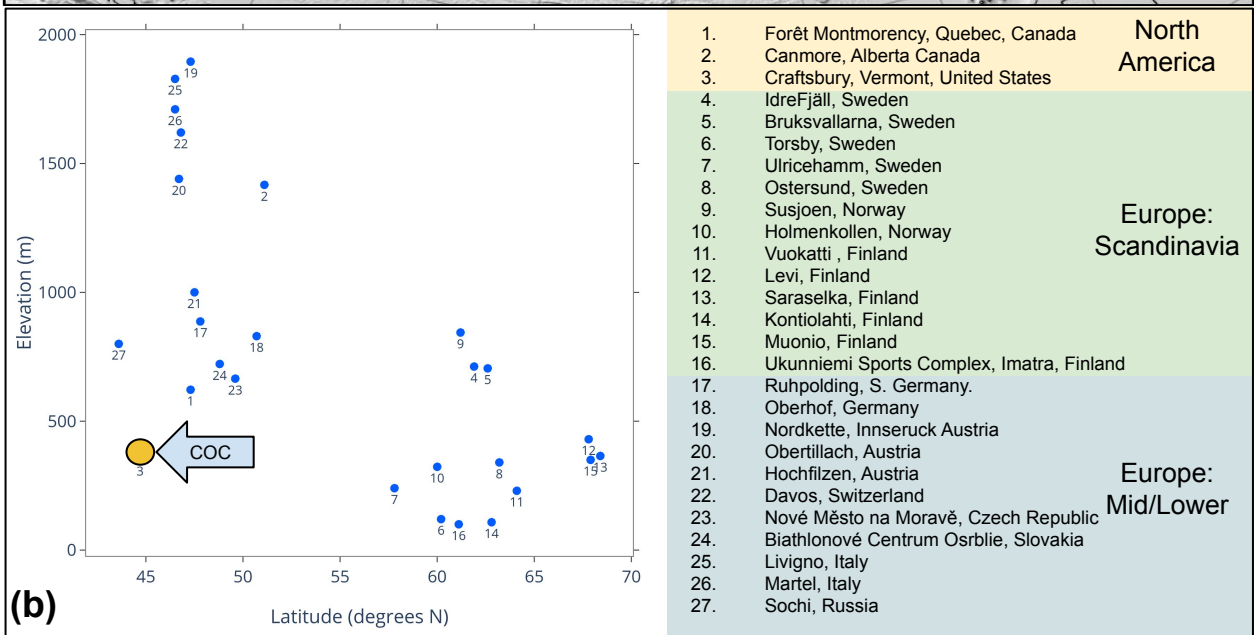

1.	Forêt Montmorency, Quebec, Canada	North America
2.	Canmore, Alberta Canada	
3.	Craftsbury, Vermont, United States	
4.	IdreFjäll, Sweden	Europe: Scandinavia
5.	Bruksvallarna, Sweden	
6.	Torsby, Sweden	
7.	Ulricehamm, Sweden	
8.	Ostersund, Sweden	
9.	Susjoen, Norway	
10.	Holmenkollen, Norway	
11.	Vuokatti , Finland	
12.	Levi, Finland	
13.	Saraselka, Finland	
14.	Kontiolahti, Finland	
15.	Muonio, Finland	
16.	Ukunniemi Sports Complex, Imatra, Finland	
17.	Ruhpolding, S. Germany.	Europe: Mid/Lower
18.	Oberhof, Germany	
19.	Nordkette, Innseruck Austria	
20.	Obertillach, Austria	
21.	Hochfilzen, Austria	
22.	Davos, Switzerland	
23.	Nové Město na Moravě, Czech Republic	
24.	Biathlonové Centrum Osrblie, Slovakia	
25.	Livigno, Italy	
26.	Martel, Italy	
27.	Sochi, Russia	

Figure 1: Locations of over summer snow storage. (a) Conical projection shows known locations of over-summer snow storage at nordic ski centers. The Craftsbury Outdoor Center is highlighted with a blue arrow labeled COC. The relative elevations of ski centers are displayed as a color gradient, marked in the legend. (b) Scatterplot of same locations as shown in (a). The Craftsbury Outdoor Center (#18) is large yellow dot (COC). It is the lowest combination of altitude and latitude of any snow storage yet attempted.

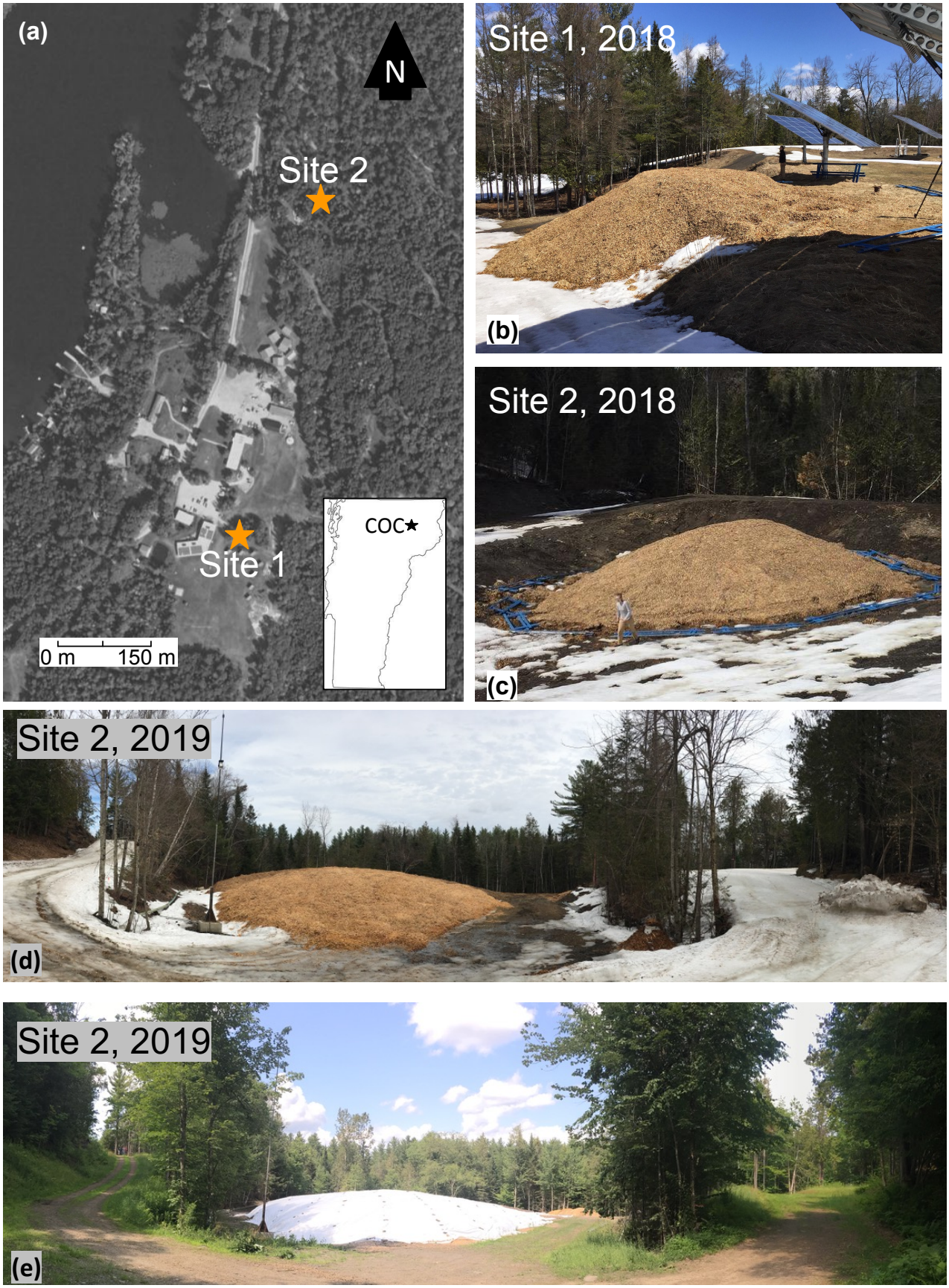

Figure 2: Snow storage at Craftsbury Outdoor Center. (a). Areal view of the Craftsbury Outdoor Center (COC) in Vermont, from http://maps.vcgi.vermont.gov. Both study site locations shown by number. (b). Site 1 (225 m^3), covered in woodchips on April 21st, 2018, with trees and solar panels for scale. (c). Site 2 (209 m^3) when installed. Site 1 received 24 m^3 of woodchips and Site 2 received 42 m^3 of woodchips. Person for scale. (d) Site 2 in April, 2019; 9271 m^3 of snow covered in 650 m^3 of woodchips, (e) Site 2 in July, 2019, the snow pile overlain by a reflective geofabric. Trees for scale.

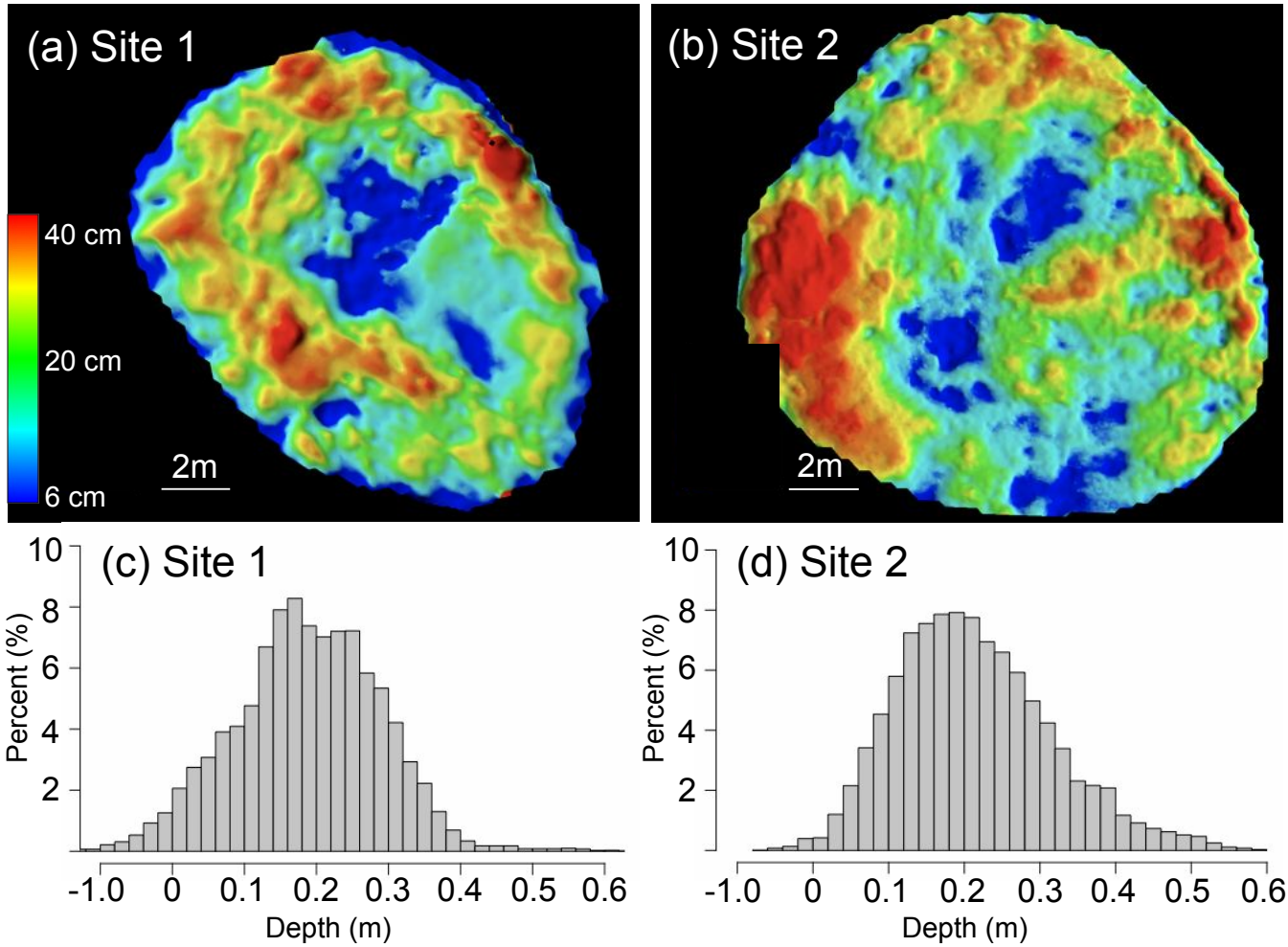

Figure 3: Wood chip thickness distribution maps of pile 1 (a) and pile 2 (b) with red indicating areas of high thickness and blue indicating areas of low thickness. Panel (c) represents the chip thickness histogram for pile 1 and (d) is chip thickness histogram for pile 2. Negative thickness values likely represent snow settling between bare snow survey and survey after wood chip emplacement.

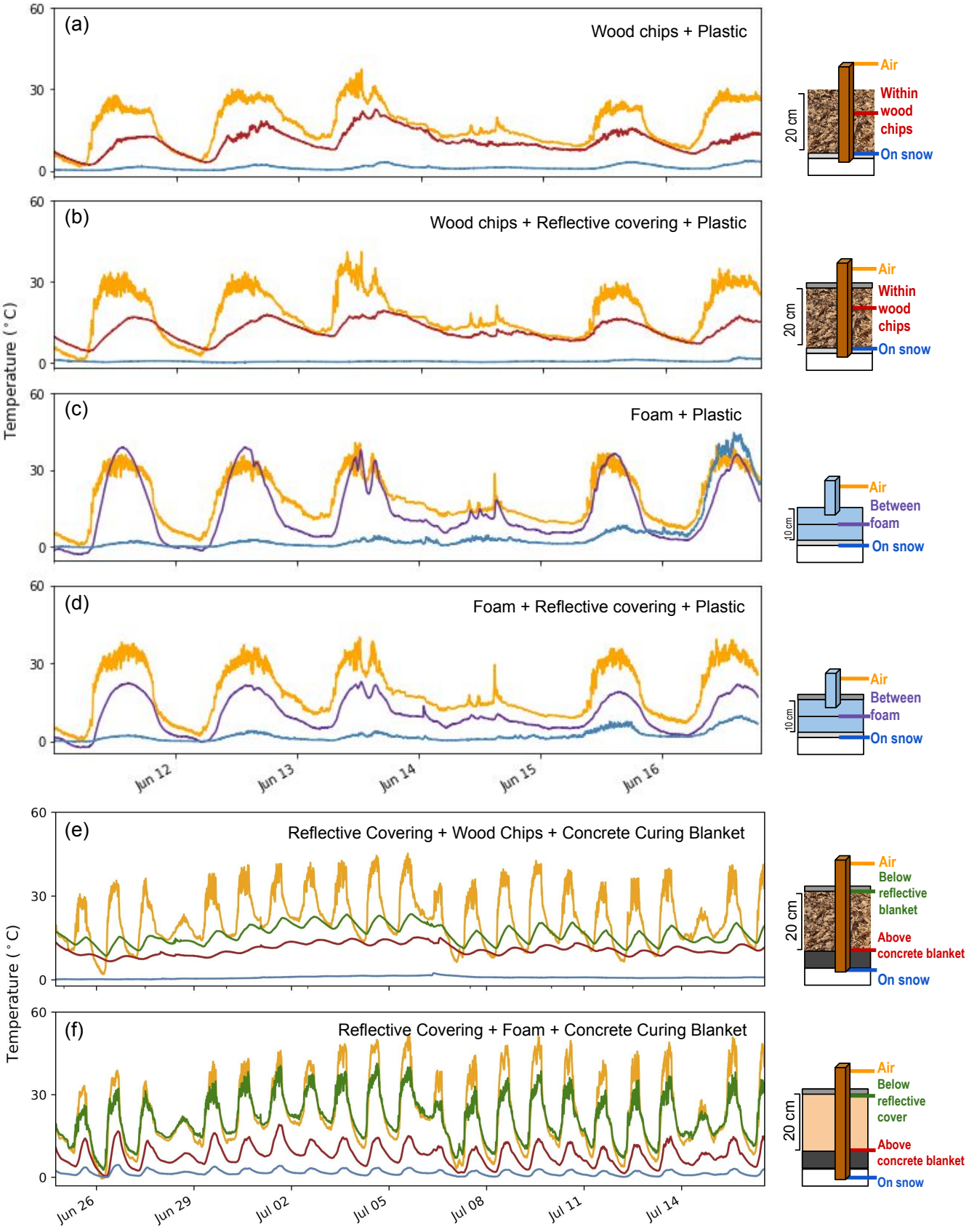

Figure 4: Cover experiments and resulting temperature records. (a) Site 1, woodchips underlain by plastic (b) Site 1, wood chips underlain by plastic and overlain by reflective cover (c) Site 1, foam underlain by plastic (d) Site 1, foam underlain by plastic and ad overlain by reflective cover (e) Site 2, woodchips underlain by concrete curing blanket and overlain by reflective cover (f) Site 2, open cell foam underlain by concrete curing blanket and overlain by reflective cover.

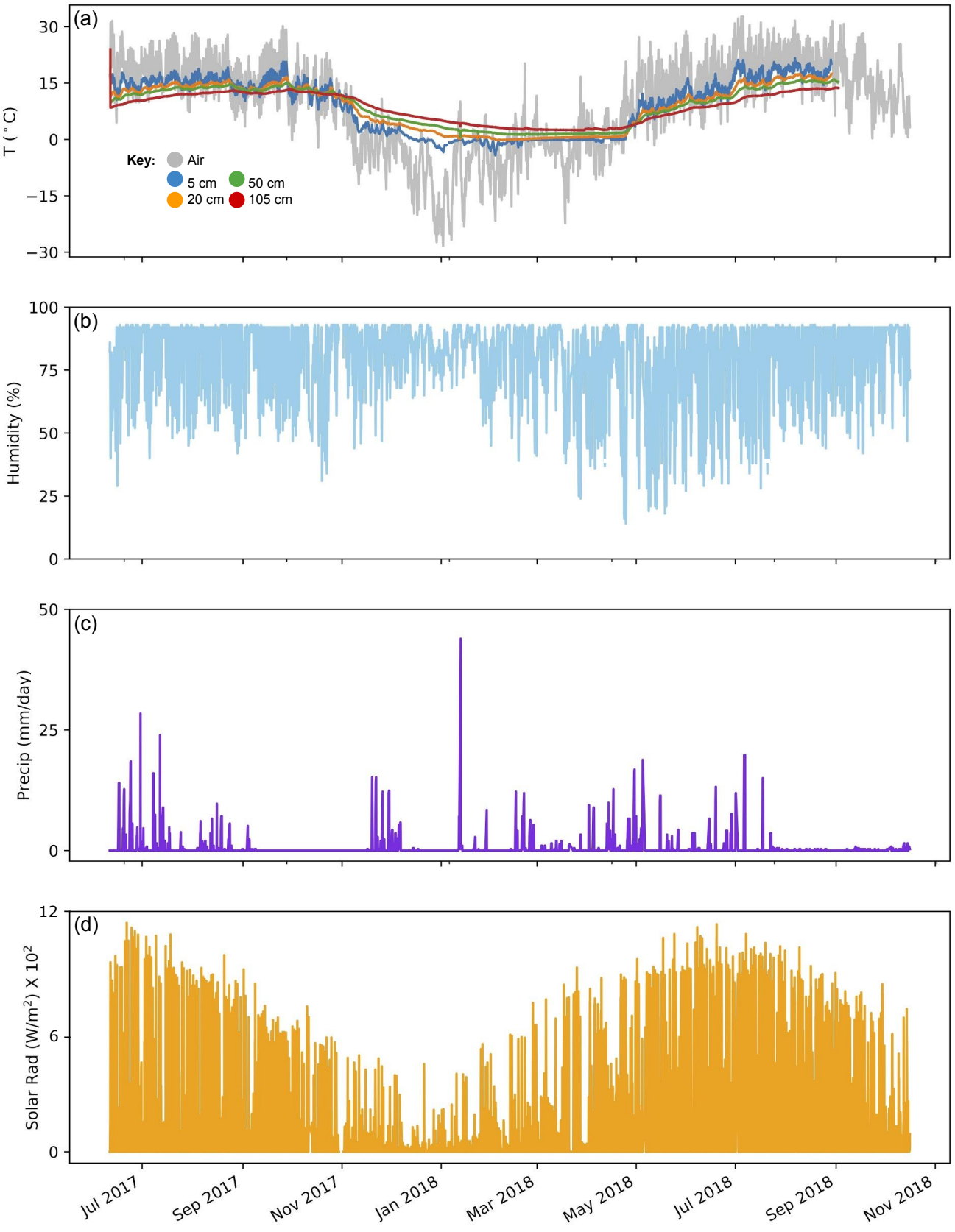

Figure 5: Meteorological conditions and soil temperature between June 11, 2017 and October 16, 2018. Weather conditions were collected by the Davis Weather station at the Craftsbury Outdoor Center near Site 2. (a) Air temperature (grey), collected at 30-minute intervals plotted with ground temperature. Ground temperature was collected at 20-minute intervals adjacent to pile 1 by four HOBO Onset dataloggers at depths below the ground surface of 5 cm (blue), 10 cm (orange), 50 cm (green), and 105 cm (red). Ground temperature record ends on September 2, 2018. (b) Relative humidity (%) (c) Precipitation (mm day^{-1}) (d) Solar radiation (W m^{-2}).

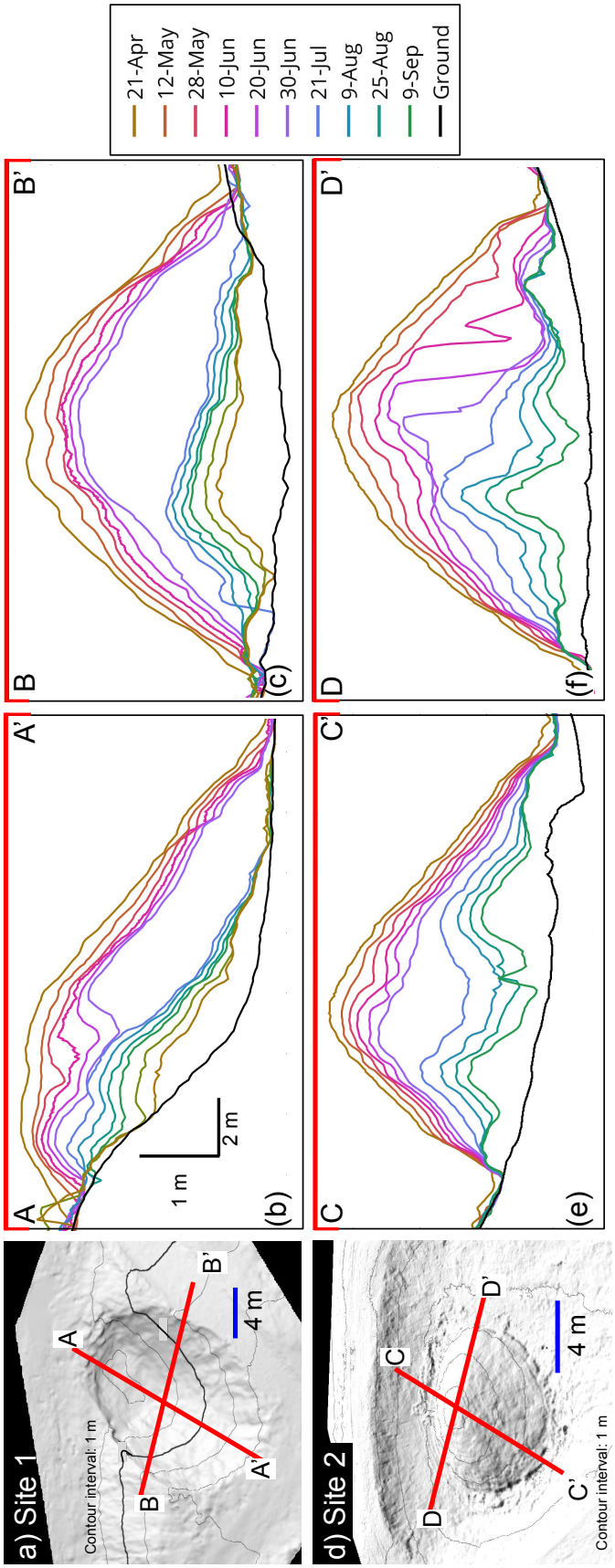

Figure 6: Snow pile topographic change over time. (a) Oblique view of digital elevation model (1 m contours) of snow pile at site 1 with cross-sections A-A' and B-B' (April 21, 2018). (b) Profiles for each terrestrial laser scan survey (April 21, 2018 to September 9, 2018, n= 13) along section A-A'. (c) Profiles for each survey along section B-B'. On July 3rd, 2018, 30 m^3 of snow was removed from the pile at site 1. (d) Oblique view of digital terrain model (1 meter contours) of snow pile at site 2 with cross-sections C-C' and D-D' (April 21, 2018). (e). Profiles for each terrestrial laser scan survey (April 21, 2018 to September 9, 2018, n= 12) along section C-C'. (f) Profiles for each survey along section D-D'. Each scan represented by a line in panels b, c, e and f.

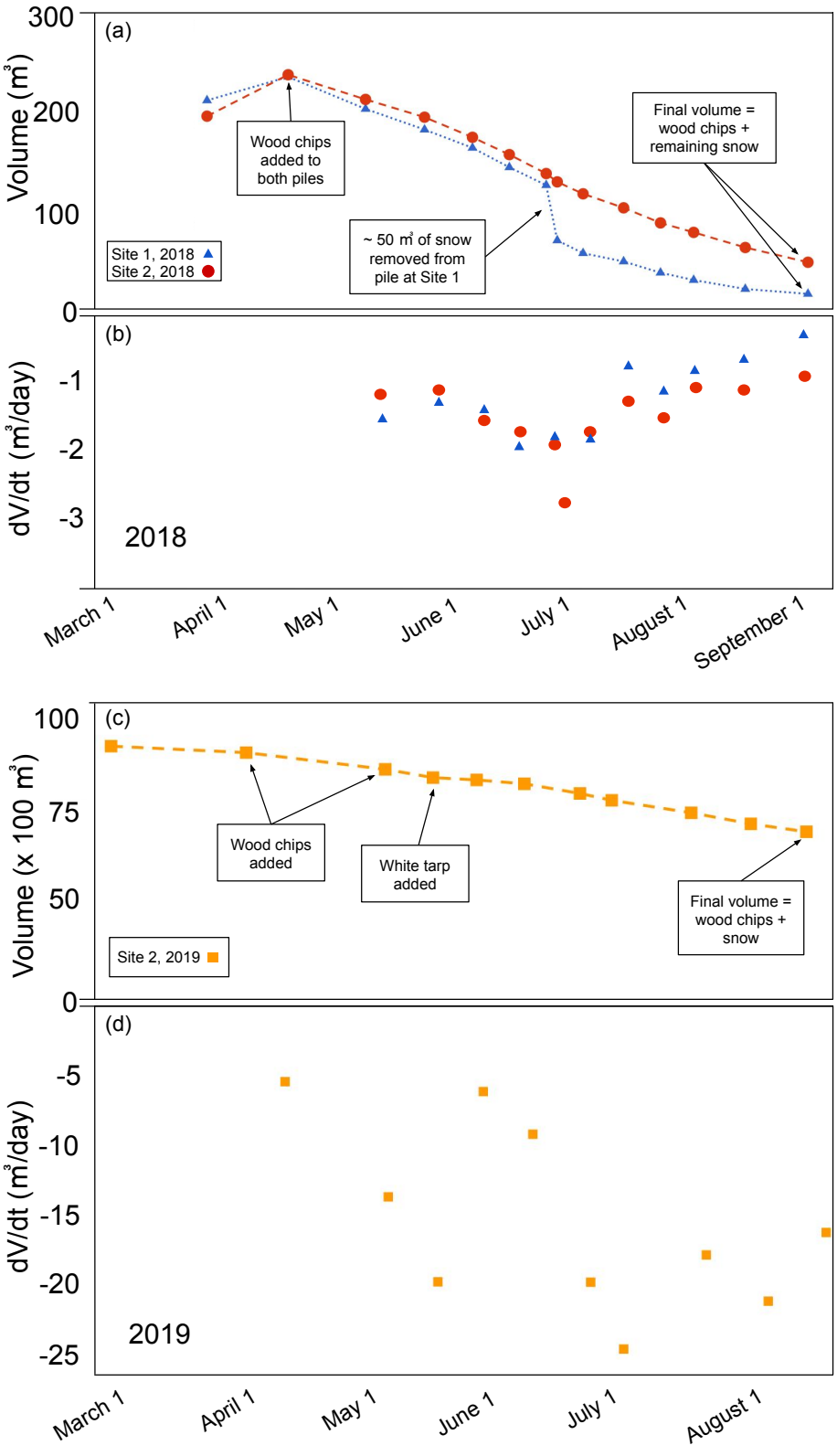

Figure 7: Volume change over time for snow piles at sites 1 and 2 measured by terrestrial laser scanning. (a) Volume of snow piles from placement in March 2018 until end of melt season in September 2018. Addition of woodchips in April and removal of snow in July at pile 1 shown by black arrows. Volumes are total including wood chips. (b) Change in volume per unit time between surveys. Rate of volume loss increases mid-summer for both piles. Site 1 received about 24 m^3 of wood chips while site 2 received about 42 m^3 of wood chips – this difference is due to pile geometry and the resulting difference in surface area. Site 1's snow pile was banked against the side of a hill while Site 2's pile was shaped like a half-sphere in the middle of an open depression. (c) Volumes of snow pile (2019) beginning March, ending September. Addition of wood chips throughout May and addition of white tarp is indicated by black arrows. Volumes include wood chip volume. (d) Change in volume per unit time between surveys.

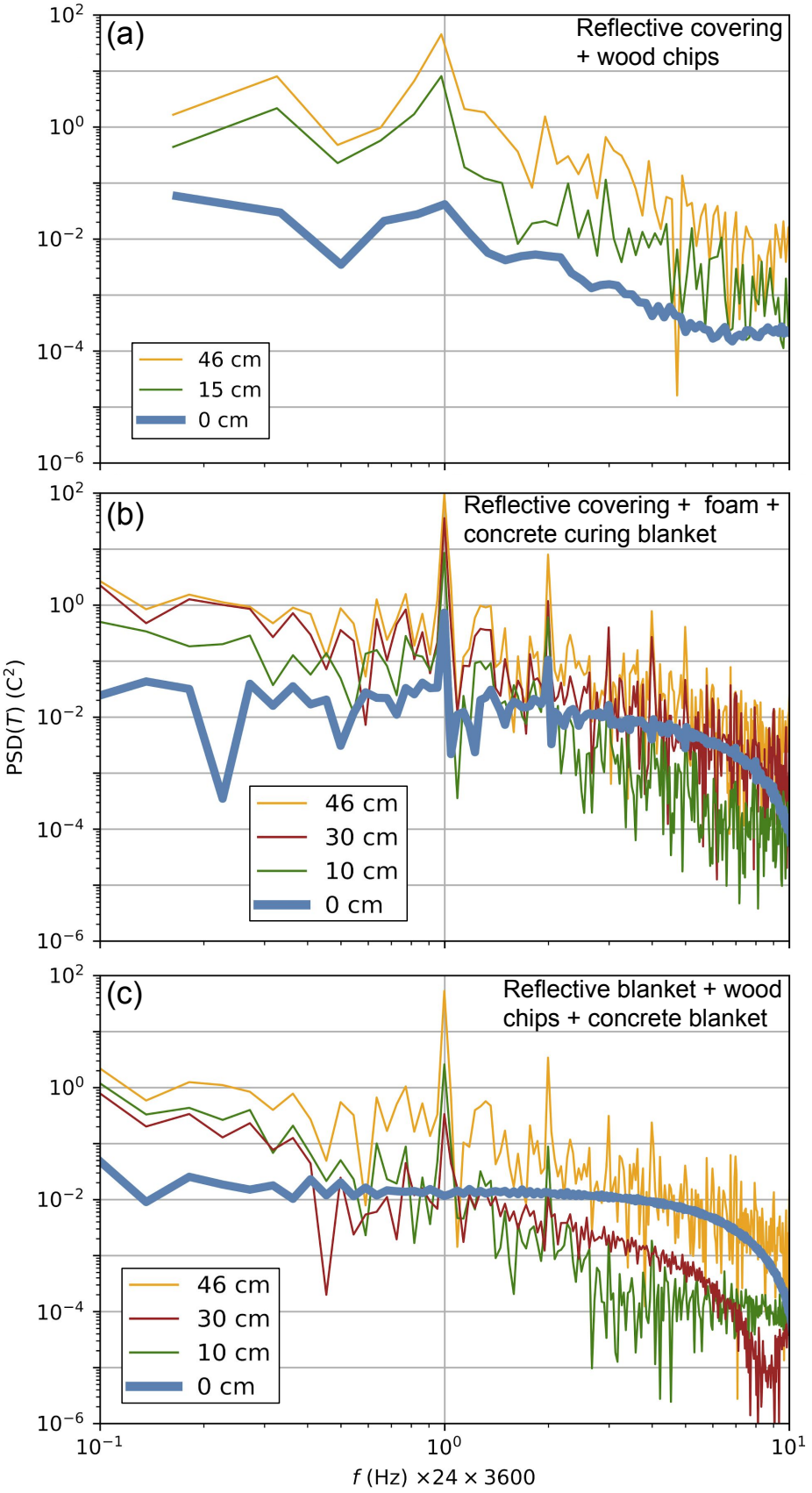

Figure 8: Power Spectral Density of temperature records from three different cover experiments (Fig. 4 b, e, and f). PSD normalizes frequency to 24 hours = 10^0 and displays the magnitude of each temperature oscillation frequency for each of four sensors per experiment (depth in cm measured below uppermost sensor). (a) experiment with wood chips and reflective cover (Fig. 4b). (b) experiment with a concrete curing blanket, open cell foam, and a reflective cover (Fig. 4f). (c) experiment with concrete curing blanket, wood chips, and a reflective cover (Fig. 4e). The lack of detectable signal (flat blue line) at snow level (0 cm) in (c) demonstrates that three layer configuration with wood chips best damps the diurnal temperature signal.